BRITISH PHARMACOLOGICAL SOCIETY

TODAY'S SCIENCE TOMORROW'S MEDICINES

Submit your abstract and register now:

CELL SIGNALLING 2020

20 – 21 April 2020
Stamford Court, University of Leicester, Leicester, UK

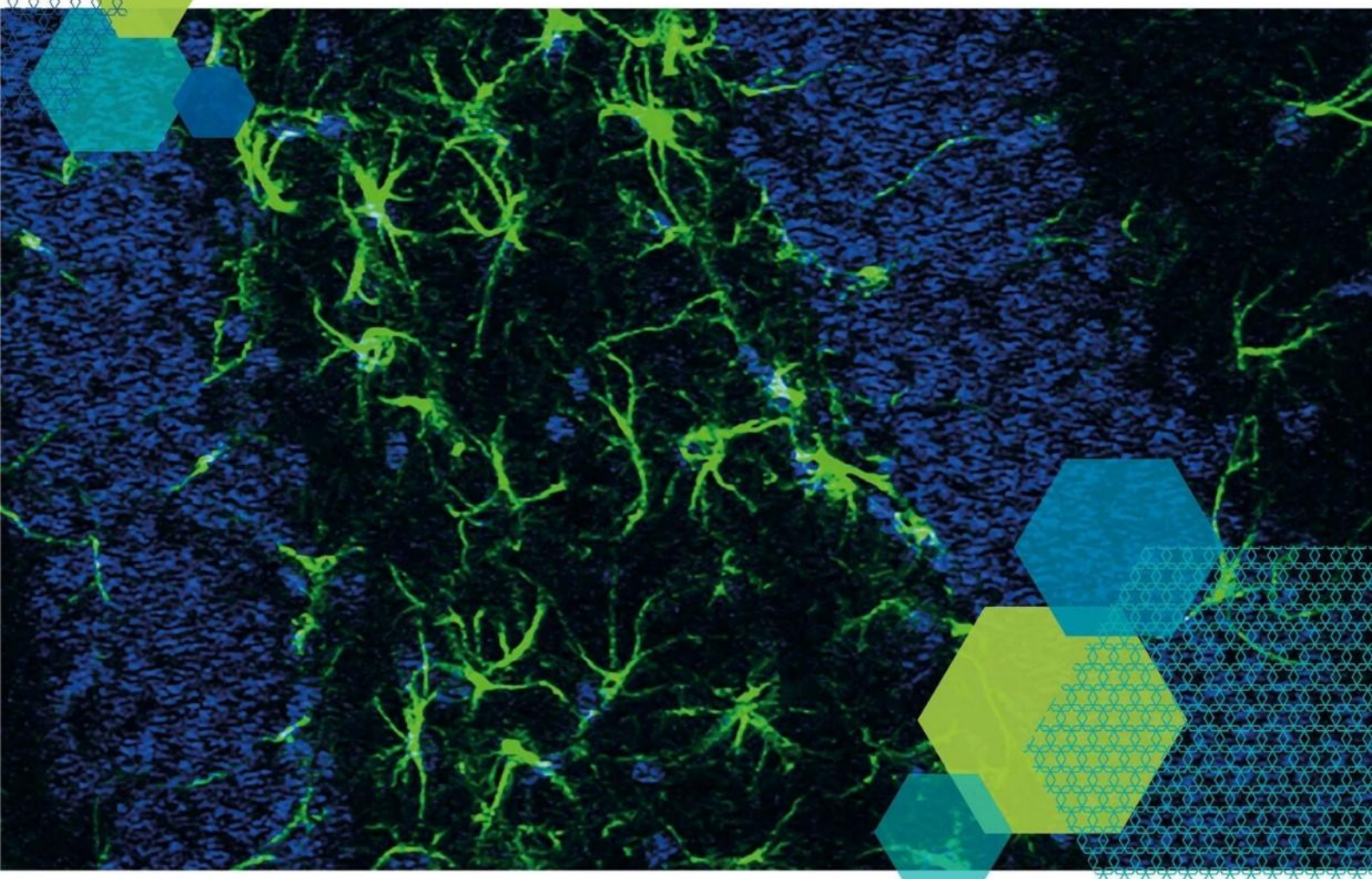

Registration details:

	Early bird	Standard
Member registration	£250	£285
Student registration	£150	£185
Non-member registration	£280	£305
Non-member student registration	£170	£195
Printed programme booklet	£10	£10

Abstract submission deadline:	Friday 31 January 2020
Member bursary deadline:	Friday 31 January 2020
Early bird registration deadline:	Friday 6 March 2020

For more information about attending or presenting please contact: meetings@bps.ac.uk or visit: www.bps.ac.uk/cell-signalling

BJP British Journal of Pharmacology

DOI:10.1111/bph.13159
www.brjpharmacol.org

RESEARCH PAPER

A Sativex®-like combination of phytocannabinoids as a disease-modifying therapy in a viral model of multiple sclerosis

A Feliú[1,2], M Moreno-Martet[2,3,4], M Mecha[1,2], F J Carrillo-Salinas[1,2], E de Lago[2,3,4], J Fernández-Ruiz[2,3,4] and C Guaza[1,2]

[1]*Neuroimmunology Group, Functional and Systems Neurobiology Department, Instituto Cajal, Consejo Superior de Investigaciones Científicas, Madrid, Spain,* [2]*Instituto Ramón y Cajal de Investigación Sanitaria, Madrid, Spain,* [3]*Department of Biochemistry and Molecular Biology, Faculty of Medicine, Complutense University, Madrid, Spain, and* [4]*Centro de Investigación Biomédica en Red sobre Enfermedades Neurodegenerativas, Madrid, Spain*

Correspondence
Carmen Guaza, Neuroimmunology Group, Functional and Systems Neurobiology Department, Instituto Cajal (Consejo Superior de Investigaciones Científicas), Avenida Doctor Arce 37, 28002, Madrid, Spain. E-mail: cgjb@cajal.csic.es

Received
3 December 2014
Revised
5 March 2015
Accepted
24 March 2015

BACKGROUND AND PURPOSE

Sativex® is an oromucosal spray, containing equivalent amounts of Δ^9-tetrahydrocannabinol (Δ^9-THC) and cannabidiol (CBD)-botanical drug substance (BDS), which has been approved for the treatment of spasticity and pain associated to multiple sclerosis (MS). In this study, we investigated whether Sativex may also serve as a disease-modifying agent in the Theiler's murine encephalomyelitis virus-induced demyelinating disease model of MS.

EXPERIMENTAL APPROACH

A Sativex-like combination of phytocannabinoids and each phytocannabinoid alone were administered to mice once they had established MS-like symptoms. Motor activity and the putative targets of these cannabinoids were assessed to evaluate therapeutic efficacy. The accumulation of chondroitin sulfate proteoglycans (CSPGs) and astrogliosis were assessed in the spinal cord and the effect of Sativex on CSPGs production was evaluated in astrocyte cultures.

KEY RESULTS

Sativex improved motor activity – reduced CNS infiltrates, microglial activity, axonal damage – and restored myelin morphology. Similarly, we found weaker vascular cell adhesion molecule-1 staining and IL-1β gene expression but an up-regulation of arginase-1. The astrogliosis and accumulation of CSPGs in the spinal cord in vehicle-infected animals were decreased by Sativex, as was the synthesis and release of CSPGs by astrocytes in culture. We found that CBD-BDS alone alleviated motor deterioration to a similar extent as Sativex, acting through PPARγ receptors whereas Δ^9-THC-BDS produced weaker effects, acting through CB_2 and primarily CB_1 receptors.

CONCLUSIONS AND IMPLICATIONS

The data support the therapeutic potential of Sativex to slow MS progression and its relevance in CNS repair.

Abbreviations

Δ^9-THC-BDS, Δ^9-tetrahydrocannabinol-botanical drug substance; Arg-1, arginase-1; CBD-BDS, cannabidiol-botanical drug substance; CSPGs, chondroitin sulfate proteoglycans; ECM, extracellular matrix; GAG chains, glycosaminoglycan chains; OPCs, oligodendrocyte precursor cells; TMEV-IDD, Theiler's murine encephalomyelitis virus-induced demyelinating disease; VCAM-1, vascular cell adhesion molecule-1; Sativex, Sativex-like combination of phytocannabinoids; XT-I, xylosyltransferase-I

Tables of Links

TARGETS
GPCRs[a]
CB_1 receptors
CB_2 receptors
Nuclear hormone receptors[b]
PPAR-γ
Enzymes[c]
Arg-1, arginase 1

LIGANDS
AM251
AM630
CBD, cannabidiol
IFN-γ
IL-10
T0070907
TNF-α
Δ9-THC, Δ9-tetrahydrocannabinol-

These Tables list key protein targets and ligands in this article which are hyperlinked to corresponding entries in http://www.guidetopharmacology.org, the common portal for data from the IUPHAR/BPS Guide to PHARMACOLOGY (Pawson *et al.*, 2014) and are permanently archived in the Concise Guide to PHARMACOLOGY 2013/14 ([a,b,c]Alexander *et al.*, 2013a,b,c).

Introduction

Multiple sclerosis (MS), the most common cause of neurological disability in young adults, is a complex autoimmune disease characterized by inflammation, demyelination and axonal damage (Compston and Coles, 2008). Most patients with MS initially develop a relapsing-remitting disease course that it is followed by a secondary progressive clinical form. By contrast, 10–15% of MS patients develop a primary progressive form from the onset of the disease. Nevertheless, effective treatments for patients with either primary or secondary MS remain elusive. Theiler's murine encephalomyelitis virus-induced demyelinating disease (TMEV-IDD) is a well-established model of MS (Lipton and Dal Canto, 1976) that is unique in reproducing the putative viral aetiology of MS and for studying virus-induced autoimmunity (Miller *et al.*, 1997). TMEV is a single-stranded RNA virus, which when inoculated intracranially in susceptible mouse strains, provokes the development of a chronic-progressive demyelinating disease. Moreover, as TMEV-IDD progresses, epitope spreading produces T-cell responses against myelin peptides.

The cannabinoids are currently being studied for their potential benefits in the treatment of MS and other neuroinflammatory/neurodegenerative diseases (Pryce and Baker, 2012; Velayudhan *et al.*, 2014). Preclinical studies have demonstrated that cannabinoids can alleviate MS-associated symptoms, such as spasticity (Baker *et al.*, 2000), and they exhibit anti-inflammatory (Arévalo-Martín *et al.*, 2003; Croxford and Miller, 2003), antioxidant, anti-excitotoxic and neuroprotective properties (Pryce *et al.*, 2003; Fernández-Ruiz *et al.*, 2010; Loría *et al.*, 2010). Cannabinoids are also protective to oligodendrocytes *in vitro* and *in vivo* (Molina-Holgado *et al.*, 2002; Gómez *et al.*, 2010; Mecha *et al.*, 2012). Sativex® is an oromucosal spray that contains an equimolecular combination of Δ^9-tetrahydrocannabinol-botanical drug substance (Δ^9-THC-BDS) and cannabidiol-botanical drug substance (CBD-BDS) and it has been approved for use in patients with MS-related spasticity and neuropathic pain. Indeed, safety studies with Sativex have indicated a low risk for serious adverse drug reactions (Serpell *et al.*, 2013). Evidence for a neuroprotective effect of Sativex was recently reported in inflammatory models of Huntington disease and in a transgenic murine model of amyotrophic lateral sclerosis (Valdeolivas *et al.*, 2012; Moreno-Martet *et al.*, 2014). Moreover, both components of Sativex have been described to independently modify immune responses in MS animal models (Maresz *et al.*, 2007; Kozela *et al.*, 2011; Mecha *et al.*, 2013b). However, there are still no clinical studies that have investigated the potential of Sativex as a disease-modifying treatment for progressive MS.

The potential of cannabinoids to influence the progression of MS also includes the possibility that they may be used for repair processes. In MS, repair and remyelination occur in shadow plaques (Chang *et al.*, 2012) but, as the disease progresses, remyelination becomes less efficient (Chang *et al.*, 2002; Franklin, 2002; Goldschmidt *et al.*, 2009). It is unlikely that the inability to remyelinate results from the absence of oligodendrocyte precursor cells (OPCs) in the adult CNS, as OPCs are present in elderly patients even decades after having been diagnosed with the disease (Chang *et al.*, 2012). Alternatively, the failure in remyelination might reflect changes in the local extracellular environment, specifically those affecting the extracellular matrix (ECM) proteins and chondroitin sulfate proteoglycans (CSPGs). Post-injury deposition of CSPGs may be a protective CNS response to limit damage (Silver and Miller, 2004), yet CSPGs up-regulation in chronic MS provokes scar formation (Sobel and Ahmed, 2001; Mohan *et al.*, 2010), which inhibits both axon regeneration and remyelination (Siebert and Osterhout, 2011; Lau *et al.*, 2012). This is why CSPGs and hyaluronan are considered to be inhibitory molecules, the accumulation of which is thought to be the main reason for the failure of remyelination (Harlow and Macklin, 2014).

TMEV represents a suitable model to elucidate the role of glial scar formation in chronic inflammatory and demyelinating CNS lesions. Chronic demyelination in the TMEV model is accompanied by alterations in spinal cord ECM and astrogliosis (Haist *et al.*, 2012) which in turn contribute to the failure in regeneration. Accordingly, limited remyelination in TMEV has been associated with insufficient oligodendroglial differentiation (Ulrich *et al.*, 2008). While cannabinoids have been shown to improve remyelination (Arévalo-Martín *et al.*,

2003), there is a little information about their effects on the ECM and CSPGs.

Thus, we set out to investigate the therapeutic potential of a Sativex-like combination of phytocannabinoids (Sativex) as a disease-modifying therapy in a model of primary progressive MS. TMEV-infected mice with established symptomatology were treated with Sativex or individual Δ^9-THC-BDS or CBD-BDS, which improved the motor deficits associated with the disease. Indeed, Sativex reduced cellular infiltrates, decreased microglial activity and diminished axonal damage in the TMEV-infected mice. Moreover, myelin morphology was restored and the expression of proinflammatory cytokines and adhesion molecules were down-regulated by Sativex. Astrogliosis, the accumulation of CSPGs and the expression of the synthetic enzyme xylosyltransferase-I (XT-I), was also reduced by Sativex treatment. In addition, our results support the involvement of CB_1 and CB_2 receptors in the beneficial effects of Δ^9-THC-BDS and of PPARγ receptors in the effects of CBD-BDS in TMEV-IDD.

Methods

Animals and Theiler's virus infection

All animal care and experimental procedures were performed in accordance with EU (2010/63/EU) and governmental guidelines (Royal Decree 53/2013 BOE n°34 and Comunidad de Madrid: ES 280790000184) and were approved by the Ethics Committee on Animal Experimentation of the Cajal Institute (CSIC) (protocol number: 2013/03 CEEA-IC). All studies involving animals are reported in accordance with the ARRIVE guidelines for reporting experiments involving animals (Kilkenny *et al.*, 2010; McGrath *et al.*, 2010). A total of 90 animals were used in the experiments described here.

TMEV-IDD-susceptible female SJL/J mice from Harlan (Barcelona, Spain) were maintained at our in-house colony (Cajal Institute, Madrid, Spain) on a 12 h light/dark cycle with *ad libitum* access to food and water. Four-week-old mice were intracerebrally inoculated in the right hemisphere with 2×10^6 plaque forming units of the Daniel strain of TMEV diluted in 30 µL of DMEM supplemented with 10% FCS (Lledó *et al.*, 1999). Sham-operated mice received 30 µL of DMEM + 10% FCS alone.

Pharmacological treatments

Sham or TMEV-IDD mice were treated daily with vehicle alone or a 1:1 combination of botanical extracts enriched with either Δ^9-THC botanical extract (Δ^9-THC-BDS) containing 67.1% Δ^9-THC, 0.3% CBD, 0.9% cannabigerol, 0.9% cannabichromene and 1.9% other phytocannabinoids or CBD: CBD botanical extract (CBD-BDS) containing 64.8% CBD, 2.3% Δ^9-THC, 1.1% cannabigerol, 3.0% cannabichromene and 1.5% other phytocannabinoids (kindly provided by GW Pharmaceuticals Ltd., Cambridgeshire, UK). The dose of Sativex administered was 10 $mg \cdot kg^{-1}$ which corresponds to 5 $mg \cdot kg^{-1}$ of Δ^9-THC-BDS plus 5 $mg \cdot kg^{-1}$ of CBD-BDS. Cannabinoids were prepared in a Tween-80 saline solution (1:16) gassing it with N_2 to avoid oxidation and they were administered i.p. once daily from days 70 to 80 post-infection when the signs of disease were evident. The duration of the treatment was based on previous studies using the TMEV-IDD model (Docagne *et al.*, 2007). Additional groups of mice received Δ^9-THC-BDS (5 $mg \cdot kg^{-1}$) or CBD-BDS (5 $mg \cdot kg^{-1}$) administered separately. In an additional experiment, mice treated with Δ^9-THC-BDS also received the CB_1 receptor antagonist AM251 (2 $mg \cdot kg^{-1}$) or the CB_2 receptor antagonist AM630 (2 $mg \cdot kg^{-1}$) (Tocris Bioscience, Bristol, UK) 30 min previously, whereas mice administered with CBD-BDS were treated 30 min beforehand with the PPARγ inhibitor T0070907 (5 $mg \cdot kg^{-1}$) (Cayman Chem, Ann Arbor, MI, USA). In all experiments and after 10 days of treatment, the motor activity was evaluated and the animals were killed with an overdose of anaesthetic for tissue collection.

Spontaneous motor activity

Locomotor activity was evaluated in mice using an activity cage (Activity Monitor System, Omnitech Electronics Inc., Columbus, OH, USA) coupled to a digiscan analyser. The number of times that the animals broke the horizontal or vertical sensor beams was measured in two 5 min sessions.

Tissue processing

Mice were anaesthetized with pentobarbital (Dolethal, 50 $mg \cdot kg^{-1}$ body weight, i.p.) and perfused transcardially. The spinal cord was fixed overnight in 4% paraformaldehyde (PFA) prepared in 0.1 M phosphate buffer (PB) and cryoprotected in sucrose solution in 0.1 M PB (15% followed by a 30%). Coronal and longitudinal spinal cord cryostat sections (15 and 30 µm thick; cryostat Leica Microsystems CM1900, Barcelona, Spain) were then processed for immunohistochemistry.

Immunohistochemistry

Free-floating spinal cord cryostat sections were washed with 0.1 M phosphate buffer (PB), PB + 0.2% Triton X-100 (PBT) and then blocked for 1 h at room temperature in blocking buffer (PBT and 5% normal goat serum: Vector Laboratories, Inc., Burlingame, CA, USA) after inhibiting the endogenous peroxidase for 3,3′ diaminobenzidine tetrahydrochloride (DAB) staining. The sections were then incubated overnight at 4°C with the primary antibody (Table 1). For colourimetric immunohistochemistry, microglial cells in spinal cord sections (30 µm thick) were stained with Iba-1 in blocking buffer. T lymphocytes were stained for CD4 and CD8 expression. We also assessed vascular cell adhesion molecule-1 (VCAM-1) staining. For immunofluorescence, SMI32 antibody was used to detect axonal damage (sections of 15 µm thick). In longitudinal and transversal 30 µm sections, axons were stained with Neurofilament-H and RIP antibodies. Astrocytes were stained with GFAP antibody, proliferative astrocyte CSPGs were stained with vimentin antibody and CSPGs with an anti-chondroitin sulfate antibody (CS56). After incubation with the primary antibody, the sections were rinsed with PBT and were incubated for 1 h with biotinylated antibodies (Vector Laboratories, Inc.). For immunofluorescence, an Alexa 488 Fluor-conjugated goat anti-rabbit antibody (for Neurofilament-H), goat anti-mouse antibody (for SMI-32 and GFAP; Molecular Probes Inc., Eugene, OR, USA) and Texas Red-conjugated donkey anti-mouse IgM (for CS56; Jackson Immunoresearch Europe, Suffolk, UK) were used. For DAB

Table 1

Primary antibodies used for immunochemistry and Western blot analysis

Antibody	Host	Dilution	Source
Iba-1	Rabbit	1:1000	Wako, Osaka, Japan
CD4	Rat IgG	1:1000	Pharmingen, San Diego, CA, USA
CD8	Rat IgG	1:1000	Pharmingen, San Diego, CA, USA
VCAM-1	Mouse IgG	1:500	DSHB, University of Iowa, Ames, IA, USA
SMI32	Mouse IgG	1:1000	Covance, Emeryville, CA, USA
Neurofilament-H	Rabbit IgG	1:1000	Millipore, Billerica, MA, USA
RIP	Mouse IgG	1:1000	DSHB, University of Iowa, Ames, IA, USA
GFAP	Mouse IgG	1:1000	Sigma-Aldrich; St Louis, MO, USA
Vimentin	Mouse IgG	1:500	Abcam, Cambridge, UK
CS56	Mouse IgM	1:250	DSHB, University of Iowa, Ames, IA, USA
Neurocan-1F6	Mouse IgG	1:500/1:1000 (Western blot)	DSHB, University of Iowa, Ames, IA, USA
	Mouse IgG	1:10000	Sigma-Aldrich, St Louis, MO, USA

Table 2

The primer sequences used in quantitative PCRs

Genes	Forward	Reverse
TNF-α	5′-GACTCCCCCCTCCGTCTAAG-3′	5′-CGCAGTAAAGCCCACGTTGT-3′
IL-1β	5′-TGGTGTGTGACGTTCCCATT-3′	5′-TCCATTGAGGTGGAGAGCTTTC-3′
IFN-γ	5′-GGCCATCAGCAACAACATAAGCGT-3′	5′-TGGGTTGTTGACCTCAAACTTGGC-3′
ICAM-1	5′-CACCCCAAGGACCCCAAGGAGAT-3′	5′-CGACGCCGCTCAGAAGAACCA-3′
Brevican	5′-ACCC ACC ACTCCGTAATTCC-3′	5′-CCATCCAGAACCCACGAGA-3′
XT-1	5′-GGGAATGCAGAAATGGGGGA-3′	5′-GAAGGTCAGAGGTGCGACAA-3′
18S	5′-ATGCTCTTAGCTGAGTGTCCCG-3′	5′-ATTCCTAGCTGCGGTATCCAGG-3′
CB_1 receptor	5′-CCAAGAAAAGATGACGGCAG-3′	5′-AGGATGACACATAGCACCAG-3′
CB_2 receptor	5′-TCGCTTAC ATCCTTCAGACAG-3′	5′-TCTTCCCTCCCAACTCCTTC-3′
PPARγ	5′-TCACAAGAGCTGACCCAATG-3′	5′-TGAGGCCTGTTGTAGAGCTG-3′
Arginase-1	5′-GAACACGGCAGTGGCTTTAAC-3′	5′-TGCTTAGCTCTGTCTGCTTTG-3′
IL-10	5′-TGAATTCCCTGGGTGAGAAGCTGA-3′	5′-TGGCCTTGTAGACACCTTGGTCTT-3′

immunostaining, the sections were incubated for 1 h with a biotin–peroxidase complex (Vector Laboratories, Inc.) and with the chromogen DAB (Sigma-Aldrich, St. Louis, MO, USA). In all cases, the specificity of staining was confirmed by omitting the primary antibody.

For immunocytochemistry, astrocytes maintained in culture for 48 h were fixed with PFA 4% for 20 min, incubated with blocking buffer and stained overnight at 4°C for neurocan, using an antibody that recognizes the N-terminal and full-length protein. The following day, the cells were rinsed and incubated for 1 h with Alexa 594 Fluor-conjugated goat anti-mouse antibody (Molecular Probes Inc.).

Microscopy and image analysis

Immunofluorescence images were acquired on a Leica TCS SP5 confocal microscope and for immunohistochemistry, with a Zeiss Axiocam high resolution digital colour camera. Individual optical sections were examined analysing five to six sections from at least five to six animals per group. Staining was quantified using Image J software (NIH, Bethesda, MD, USA), maintaining the threshold intensity constant to compare the experimental and control images obtained within the experiments. The data are presented as the percentage of the total area stained with respect to the sham-operated animals.

Inflammatory infiltrates analysis and Luxol fast blue (LFB) staining

The spinal cord sections were stained with haematoxylin and eosin (H&E) to analyse the infiltrates in the parenchyma and with LFB to define myelin integrity. Inflammatory infiltrates were evaluated by scoring the infiltrate in the spinal cord on

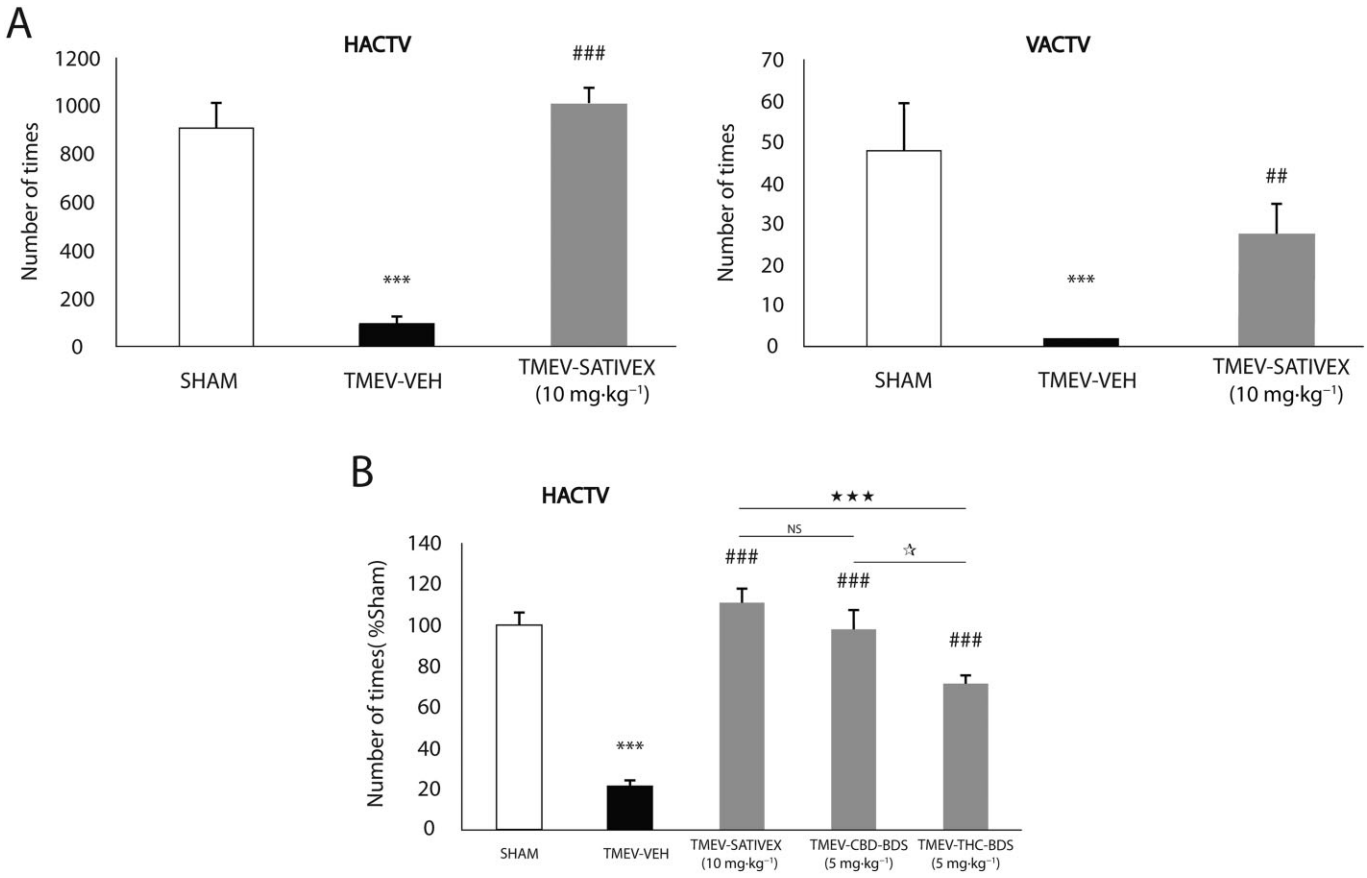

Figure 1

A Sativex®-like combination of phytocannabinoids, Δ^9-THC-BDS or CBD-BDS treatments alone, significantly improved motor deficits in the chronic phase of TMEV infection. SJL/J mice were intracranially inoculated with TMEV or the vehicle alone and after 70 days, once the symptomatology was established, the mice were treated i.p. for 10 consecutive days with a Sativex-like combination of phytocannabinoids (10 mg·kg^{-1}), CBD-BDS (5 mg·kg^{-1}), Δ^9-THC-BDS (5 mg·kg^{-1}) or the vehicle alone. On the last day of treatment, motor function was evaluated by measuring horizontal (HACTV) and vertical activity (VACTV) in the activity cage test (A) which revealed a significant attenuation of motor deficits in the TMEV-IDD model following Sativex administration. In a comparative analysis, Sativex and CBD-BDS alone were the most effective treatments as they abolished the decreased motor activity and restored the normal levels of HACTV (B). Activity parameters were recorded for 10 min and the results are represented as the mean ± SEM of nine mice per group: ***$P \leq 0.001$ versus Sham; ##$P \leq 0.01$; ###$P \leq 0.001$ versus TMEV-VEH animals; ★★★$P \leq 0.001$ versus TMEV-Sativex; ☆$P \leq 0.05$ TMEV-CBD-BDS versus TMEV-THC-BDS (non parametric Kruskal–Wallis test). NS, not significant.

a scale of 0 to 4: a score of 0 reflects the absence of infiltrates; 4 reflects the maximal infiltrate; while the intermediate scores of 1, 2 and 3 define the increasing infiltrate density in the tissue.

For LFB staining, free-floating spinal cord sections (15 µm thick) were washed with 0.1 M PB. Tissue samples were dehydrated successively in an ethanol series from 70 to 95% and the sections were then incubated in LFB solution at 56°C in an oven overnight. The following day, the excess stain was rinsed off from the sections with 95% ethanol and the slides were contrasted in lithium carbonate solution for 30 s. Finally, the sections were dehydrated, cleared with xylene and cover slipped.

Astrocyte cell cultures

Astrocyte cultures were prepared from postnatal Wistar pups (0–2 days of age) as described previously (Mecha *et al.*, 2011). After isolation, the astrocytes were plated in poly-D-lysine-coated 6-well plates at a density of 6×10^5 cells·mL^{-1} for Western blotting and PCR analysis or in 24-well plates with coverslips at a density of 5×10^4 cells·mL^{-1} for immunocytochemistry and grown in DMEM medium supplemented with 5% horse serum, 5% FBS, 100 U·mL^{-1} penicillin and 100 mg·mL^{-1} streptomycin. The medium was replaced 3 h later, adding cytosine-d-arabinofuranoside (Sigma-Aldrich). After 4 days *in vitro*, the cells were maintained for 1 h in DMEM before they were then exposed for 24, 48 or 72 h to TGFβ1 and bFGF (10 ng·mL^{-1} each; Peprotech, Rocky Hill, NJ, USA) and with Sativex (100 nM: 50 CBD-BDS + 50 Δ^9-THC-BDS; 0.50 µM: 0.25 CBD-BDS + 0.25 Δ^9-THC-BDS; 1 µM: 0.5 CBD-BDS + 0.5 Δ^9-THC-BDS) or the vehicle alone. The cells harvested at 24 h were processed for PCR analysis to analyse the mRNA expression of brevican and XT-I. Immunocytochemical studies were performed on astrocytes harvested

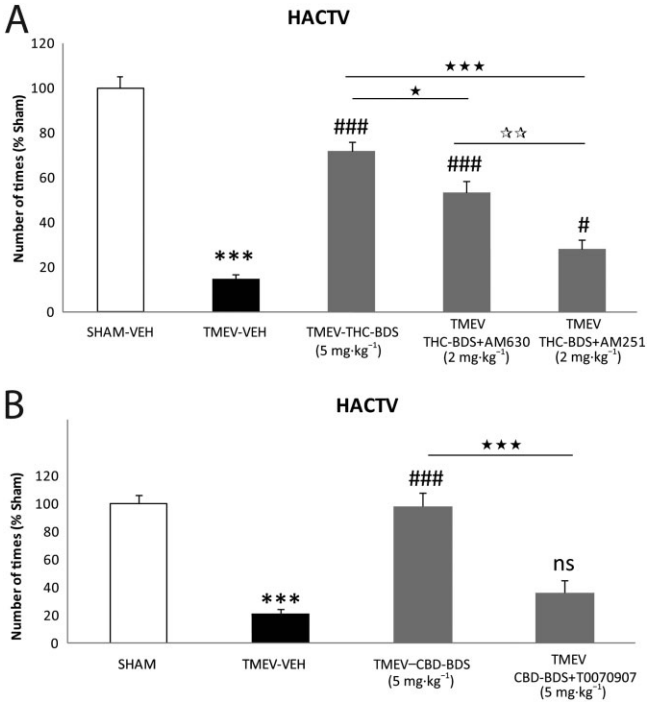

Figure 2

The involvement of the CB_1, CB_2 receptors and PPARγ in the effect of the Sativex®-like phytocannabinoid combination. To determine the receptors involved in the beneficial effects of Sativex, we administered Δ^9-THC-BDS (5 mg·kg^{-1}) together with a selective antagonist for the CB_2 receptor (AM630, 2 mg·kg^{-1}) and an antagonist of the CB_1 receptor (AM251, 2 mg·kg^{-1}). CBD-BDS (5 mg·kg^{-1}) was administered in combination with a PPARγ receptor antagonist (T0070907, 5 mg·kg^{-1}) for 10 days once the symptomatology had been established and motor function was evaluated by measuring horizontal activity (HACTV) on day 80 post-infection. The positive effect of Δ^9-THC-BDS was significantly blocked by the administration of the CB_1 receptor antagonist and less so by the CB_2 receptor antagonist (A). Likewise, the beneficial effect of CBD-BDS was significantly attenuated by the antagonist of PPARγ (B). Activity parameters were recorded for 10 min and the results represent the mean ± SEM of six mice per group: ***$P \leq 0.001$ versus Sham; #$P \leq 0.05$ ###$P \leq 0.001$ versus TMEV-VEH animals; ★$P \leq 0.05$ versus TMEV-THC-BDS; ★★★$P \leq 0.001$ versus TMEV-Δ^9-THC-BDS; versus TMEV-CBD-BDS; ☆☆$P \leq 0.01$ TMEV-THC-BDS-AM630 versus TMEV-THC-BDS-AM251 (one-way ANOVA followed by Tukey's and Bonferroni's test: CBD-BDS and antagonist analysis; non-parametric Kruskal–Wallis test: Δ^9-THC-BDS and antagonist analysis). ns, not significant.

after 48 h, whereas the supernatants were taken from cells incubated with the stimuli for 72 h. These supernatants were analysed by Western blots to evaluate the amount of ECM secreted into the medium.

Reverse transcription (RT) and real-time PCR

Total RNA was extracted from spinal cords or astrocyte cultures using RNeasy mini columns (Qiagen, Manchester, UK), avoiding genomic DNA contamination by DNase I degradation (DNase I, Sigma-Aldrich). The RNA yield was determined using a Nanodrop spectrophotometer (Thermo Scientific; Wilmington, DE, USA) and the total RNA (1 µg in 20 µL) was reverse transcribed into cDNA using poly-dT primers and a reverse transcription kit (Promega Biotech Ibérica, S.L., Madrid, Spain). Real-time PCR was carried out with SYBR® and the oligonucleotide primer sequences (Applied Biosystems, Warrington, UK) used are given in Table 2. After an initial incubation at 50°C for 2 min and 95°C for 10 min, PCR amplification was performed over 40 cycles of 95°C for 15 s and 60°C for 1 min. The samples were assayed in triplicate on an Applied Biosystems PRISM 7500 Sequence detection system. To rule out genomic DNA contamination, a control sample using RNA that had not been reversed transcribed was used as the template for each set of extractions. Gene expression was calculated using the $2^{-\Delta\Delta Ct}$ method and the relative expression was quantified by calculating the ratio between the values obtained for each gene of interest and those of the 18S gene. The results are expressed as a percentage with respect to the sham operated mice for each time point.

Supernatant protein concentration and Western blotting analysis

Identical amounts (1 mL) of astrocyte supernatant were precipitated overnight at –20°C in 4 vol acetone. The proteins were pelleted by centrifugation at 11,180× *g*, dried and resuspended in 50 µL chondroitinase ABC buffer (50 mM Tris pH 8.0, 60 mM sodium acetate, 0.02% BSA) and treated for 3 h at 37°C with 0.1 U·mL^{-1} chondroitinase ABC from *Proteus vulgaris* (Sigma-Aldrich). This reaction was stopped by adding Laemmli sample buffer and boiling for 10 min. The proteins (15 µL of the protein supernatant) were then resolved on a 6% SDS-polyacrylamide gel and transferred at 4°C to a nitrocellulose membrane (Amersham Biosciences, Piscataway, NJ, USA). The membranes were incubated for 20 min in citrate buffer at 95°C for antigen retrieval and then washed with Tris-buffered saline (TBS) followed by further washes with TBS with 0.1% Tween® 20 (TBST). The membranes were blocked for 1 h in 5% BSA (Gibco-Invitrogen S.A., Barcelona, Spain) in TBST and they were probed overnight for neurocan (Table 1). The membranes were then washed in blocking solution and incubated with a secondary HRP conjugated goat anti-mouse IgG antibody for 1 h (1:8000; Bio-Rad, Hercules, CA, USA). The membranes were washed with TBST and TBS. Protein bands were visualized by enhanced chemiluminescence detection and the amount of protein was estimated by densitometry (GS800 calibrated densitometer; Bio-Rad).

Data analysis

Data are expressed as the mean ± SEM. One-way ANOVA followed by the Bonferroni and Tukey's *post hoc* test or non-parametric Kruskal–Wallis test or unpaired two-tailed Student's *t*-test were used to determine the statistical significance. The level of significance was set at $P \leq 0.05$.

Results

The treatment with Sativex, Δ^9-THC-BDS or CBD-BDS alone significantly improved motor function in TMEV-IDD: the involvement of the CB_1, CB_2 receptors and PPARγ

We studied the effect of Sativex and of the two components, Δ^9-THC-BDS and CBD-BDS, individually in the TMEV-IDD

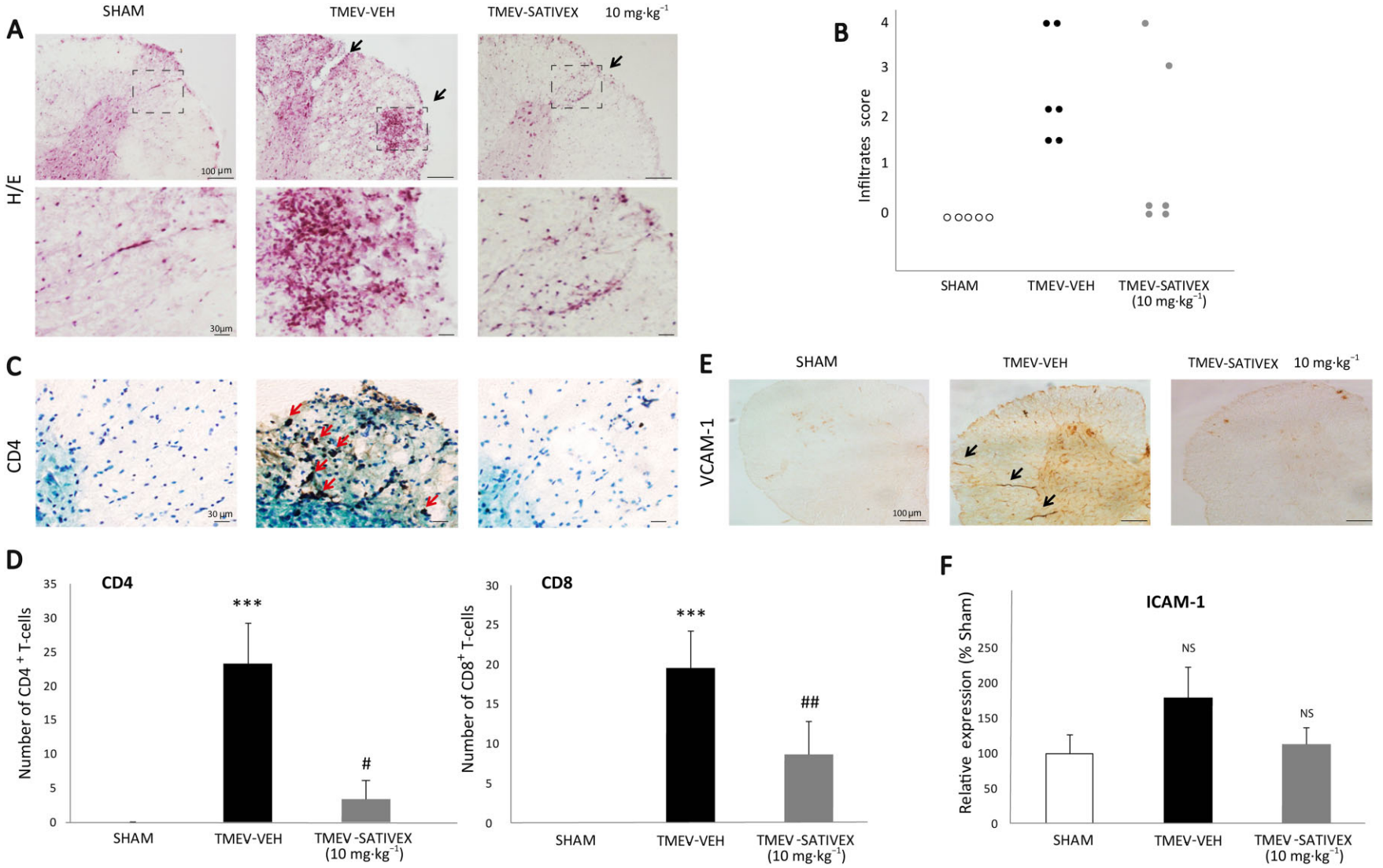

Figure 3

A Sativex®-like phytocannabinoid combination treatment decreased leukocyte infiltration and down-regulated the adhesion molecules in the spinal cord of TMEV-infected animals. Transverse cervical spinal cord sections (30 µm thick) obtained at day 80 post-infection were stained with H&E (A). TMEV infection increased leukocyte infiltration, an effect that was attenuated by Sativex (10 mg·kg^{-1}), as indicated by the infiltrate score (B) and by the analysis of CD4 and CD8 lymphocyte staining (representative microphotographs of CD4 staining, C; quantification of CD4 and CD8 number of positive cells, D). Sativex also showed a tendency to decrease mRNA expression of the ICAM-1 adhesion molecule as determined by RT-PCR on spinal cord of TMEV-infected animals ($n = 6$ per group) normalizing mRNA expression to that of the 18S gene, (F). Sativex significantly reduced the expression of VCAM-1 adhesion molecule (representative microphotographs of VCAM-1 staining, E). The data represent the mean ± SEM: ***$P \leq 0.001$ versus Sham; #$P \leq 0.05$, ##$P \leq 0.01$ versus TMEV-VEH animals (non-parametric Kruskal–Wallis test: CD4 and CD8 analysis). For histology analysis, five to six spinal cord slices per animal were analysed (n = 5–6 animals per group): Scale bar = 100 µm; 30 µm. NS, not significant.

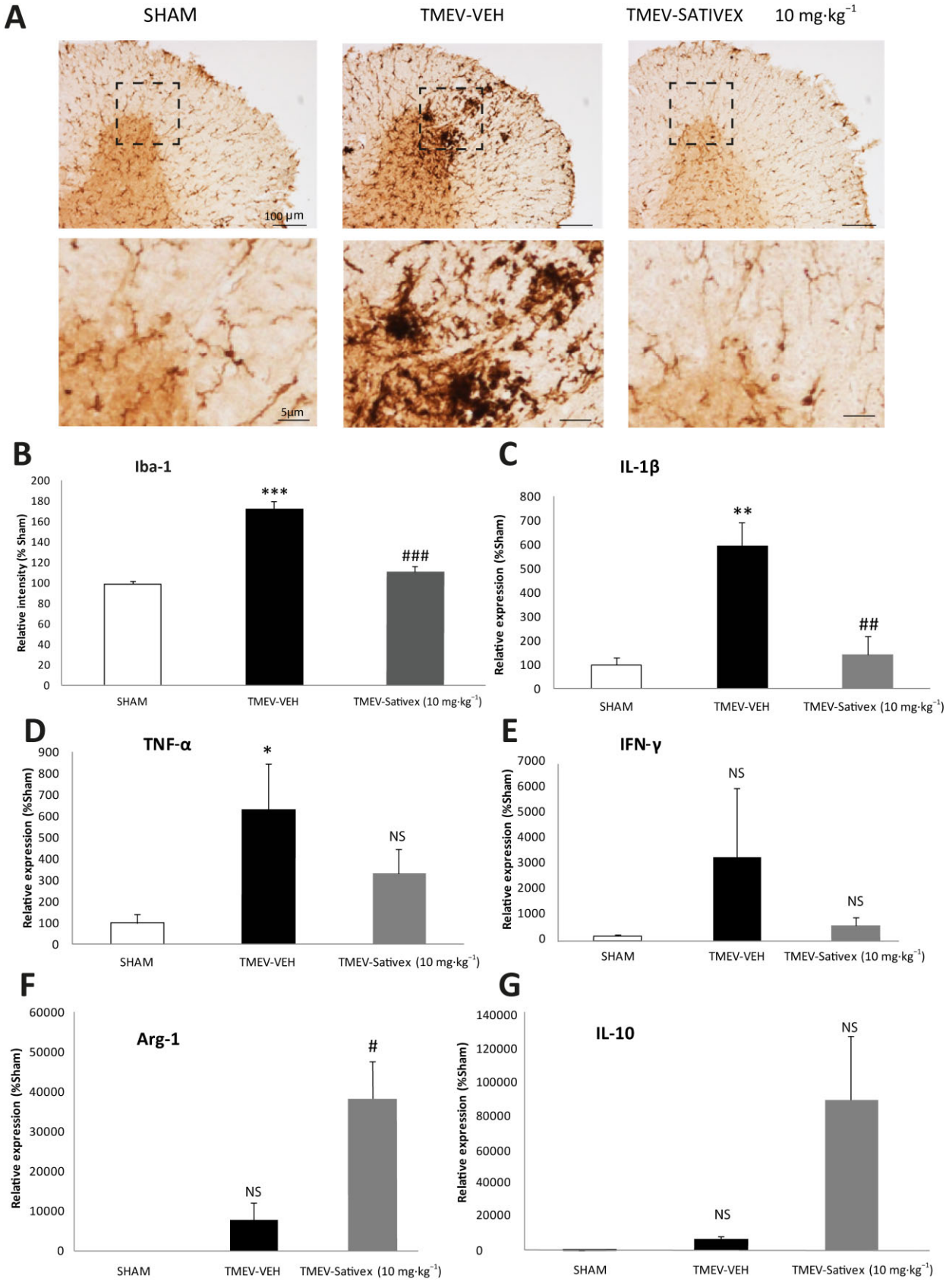
A
SHAM
TMEV-VEH
TMEV-SATIVEX 10 mg·kg⁻¹
100 µm
5µm
B
Iba-1
Relative intensity (% Sham)
***
###
SHAM
TMEV-VEH
TMEV-Sativex (10 mg·kg⁻¹)
C
IL-1β
Relative expression (%Sham)
**
##
D
TNF-α
*
NS
E
IFN-γ
NS
NS
F
Arg-1
#
NS
G
IL-10
NS
NS

model of murine primary progressive MS. To this end, 70 days after TMEV infection, mice were treated for 10 consecutive days with Sativex (10 mg·kg^{-1}: 5 mg·kg^{-1} Δ^9-THC-BDS and 5 mg·kg^{-1} CBD-BDS), with CBD-BDS (5 mg·kg^{-1}) or with Δ^9-THC-BDS (5 mg·kg^{-1}) or an equivalent amount of the vehicle alone and their motor activity was then assessed in an activity cage. As expected, TMEV infection dramatically reduced both horizontal and vertical activity in the chronic phase of the model, whereas Sativex treatment abolished these motor deficits (Figure 1A). The same degree of motor improvement was seen after the treatment with CBD-BDS alone, whereas Δ^9-THC-BDS provoked a weaker improvement (Figure 1B). These data indicate that Δ^9-THC-BDS and CBD-BDS, used independently or in combination (in a Sativex-like mixture), restored motor function in TMEV-infected mice, although a greater influence in the effect of Sativex can be attributed to CBD-BDS. These treatments had no effect on sham animals (data not shown).

The different contribution of each phytocannabinoid to the activity of Sativex may be related to differences in their potential targets. Thus, to determine how the CB_1 and CB_2 receptors influenced the effects of Δ^9-THC-BDS, this phytocannabinoid was co-administered with a selective antagonist for the CB_1 (AM251) or CB_2 (AM630) receptor. In addition, as CBD appears to act through PPARγ (Esposito *et al.*, 2011), and only negligibly through the CB_1 and CB_2 receptors (Izzo *et al.*, 2009; Mecha *et al.*, 2013b), CBD-BDS was also administered along with the PPARγ antagonist, T0070907. Our data indicated that the positive effect of Δ^9-THC-BDS on motor deterioration was significantly blocked by the CB_1 receptor antagonist AM251 and only partially by the CB_2 receptor antagonist AM630 (Figure 2A). Similarly, the beneficial effect of CBD-BDS was significantly attenuated by the PPARγ antagonist (Figure 2B). These data suggest the involvement of CB_1 receptors and, to a lesser extent, of CB_2 receptors in ameliorating the effect of motor disturbances in TMEV-IDD mice provoked by Δ^9-THC-BDS and an equivalent role of PPARγ in the effects of CBD-BDS. Moreover, we saw that Sativex treatment tended to up-regulate the gene expression of CB_1 and CB_2 receptors and of PPARγ in TMEV animals (data not shown). Accordingly, these three targets might be involved in the action of Sativex on TMEV-IDD consistent with the idea of a broad-spectrum effect of this combination of phytocannabinoids.

Sativex reduced leukocyte infiltration and expression of adhesion molecules in the spinal cord of TMEV-infected animals

H&E staining revealed that infection with TMEV provoked the infiltration of immune cells into the spinal cord (Figure 3A). Treatment with Sativex partly diminished this infiltration (Figure 3B) and specifically decreased the accumulation of CD4 and CD8 lymphocytes into the parenchyma (Figure 3C,D). Sativex also reduced the expression of VCAM-1 (Figure 3E) and ICAM-1 (Figure 3F), both involved in peripheral immune cell transmigration. These results suggest that Sativex may restrict the permissiveness of immune cell infiltration into the CNS parenchyma. Indeed, no infiltrates were detected in sham-operated mice treated with Sativex (data not shown).

Sativex decreased microglial activity, down-regulated the expression of proinflammatory cytokines and up-regulated arginase-1 (Arg-1) and IL-10 in the spinal cord of TMEV-infected mice

Microglial/macrophage activation plays a critical role in TMEV-IDD and thus, we analysed the effect of Sativex on Iba-1 immunoreactivity in the spinal cord of TMEV-infected mice. As expected, Iba-1 staining revealed increased microglial reactivity in the spinal cord at chronic phases of the disease following TMEV infection. Sativex administration significantly reduced the intensity of this microglial labelling (Figure 4A,B). Moreover, no microglia reactivity was detected in Sham mice administered Sativex (data not shown).

The reduction of microglia reactivity was accompanied by a significant reduction of IL-1β mRNA levels (Figure 4C) and a tendency to reduce TNF-α and IFN-γ (Figure 4D,E). Sativex treatment also up-regulated the expression of Arg-1 and IL-10 mRNA showed a tendency to increase (Figure 4F,G). These data suggest that Sativex could act as an immunomodulator, not only limiting the inflammation in TMEV-IDD mice but also promoting an anti-inflammatory environment. No effect on these genes was observed in Sham animals treated with the Sativex (data not shown).

Sativex restored myelin morphology and prevented the axonal damage detected in TMEV-infected mice

Demyelinated areas that are evident upon LFB staining can be observed in TMEV-IDD infected mice at chronic phases of the disease. However, demyelination was diminished in TMEV-infected mice treated with Sativex as it preserved the morphology of the myelin sheaths in these infected mice (Figure 5A). To further assess the neuroprotective potential of Sativex, we evaluated axonal damage in TMEV-infected mice, as reflected by Neurofilament-H and SMI32 staining. Axonal damage in the white matter tracts was clearly evident in the TMEV-

Figure 4

A Sativex®-like phytocannabinoid combination attenuated the microglial response, down-regulated proinflammatory cytokines and up-regulated Arg-1 and IL-10 in the chronic phases of TMEV-IDD. Transverse cervical spinal cord sections (30 μm thick) obtained at day 80 post-infection were stained for Iba-1. (A) Representative microphotographs of Iba-1 immunostaining showing morphological changes in the microglial cells of infected animals that were reversed by Sativex treatment (10 mg·kg^{-1}). (B) Quantification of the percentage area occupied by microglia in the spinal cord white matter per field (n = 5–6 animals per group). Sativex treatment also decreased IL-1β (C) TNF-α (D) and IFN-γ (E) mRNA induction and increased Arg-1 (F) and IL-10 (G) as determined by RT-PCR in the spinal cord of TMEV-infected animals, normalizing mRNA expression to that of the 18S gene (n = 6 per group). The data represent the mean ± SEM: *$P \leq 0.05$, **$P \leq 0.01$, ***$P \leq 0.001$ versus Sham; #$P \leq 0.05$, ##$P \leq 0.01$, ###$P \leq 0.001$ versus TMEV-VEH animals (one-way ANOVA followed by Tukey's and Bonferroni's test: IL-1β analysis; non-parametric Kruskal–Wallis test: Iba-1 analysis; and unpaired two-tailed Student's t-test: TNF-α and Arg-1 analysis). For histology analysis, five to six spinal cord slices were examined per animal (n = 6 animals per group): Scale bar = 100 μm; 5 μm. NS, not significant.

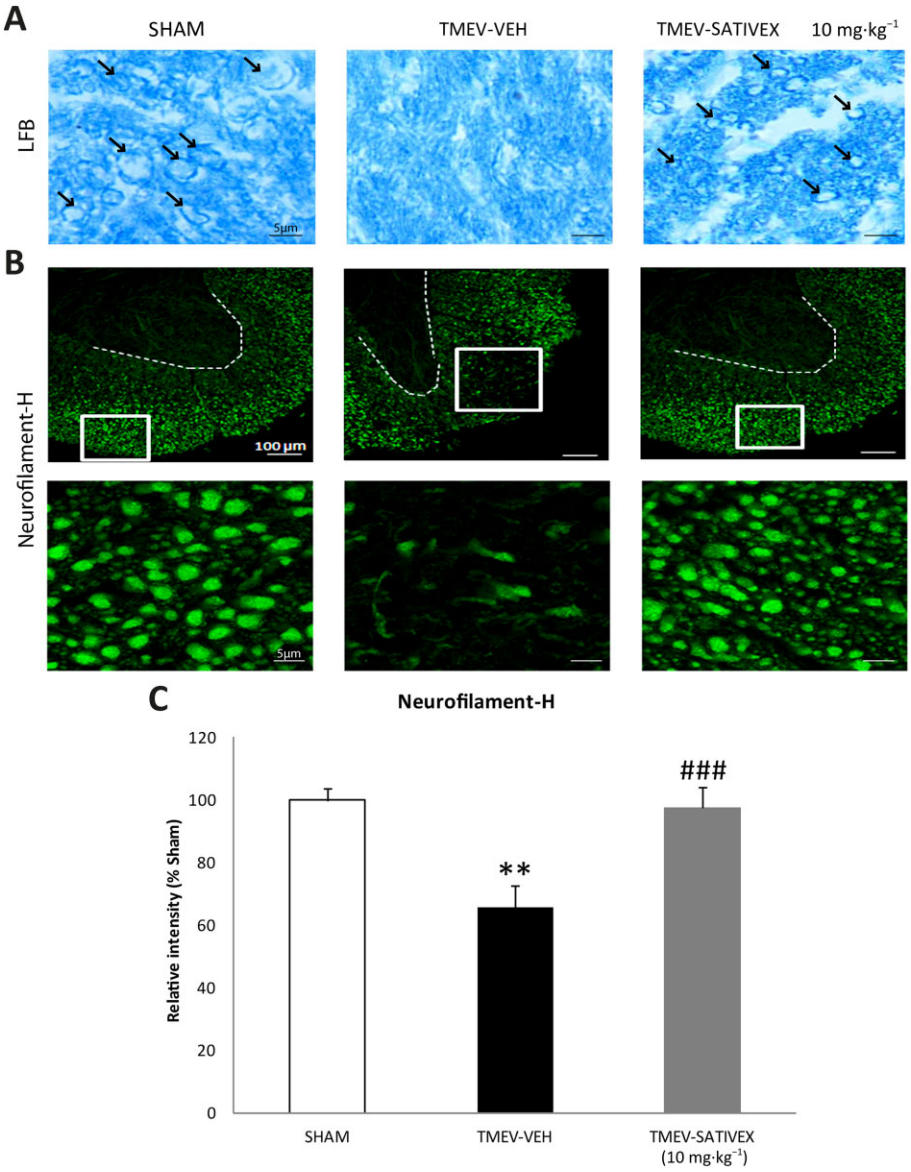

Figure 5

Sativex®-like phytocannabinoid combination treatment restored myelin morphology and prevented axonal damage in TMEV-infected mice. Transverse cervical spinal cord sections were obtained at day 80 post-infection and stained with LFB (15 µm thick) and Neurofilament-H (30 µm thick). The myelin was clearly disrupted in cervical spinal cord sections from infected animals treated with the vehicle while Sativex (10 mg·kg^{-1}) treatment contributed to maintain the myelin structure (A, arrows indicate myelin sheaths. (B) Representative images of Neurofilament-H staining showing that there is prominent axonal damage in the spinal cord white matter of vehicle-treated infected animals that diminished significantly following Sativex treatment. The area occupied by Neurofilament-H was quantified in the spinal cord white matter of each field (5–6 slices, n = 5–6 animals per group) (C). The data represent the mean ± SEM: $^{**}P \leq 0.01$ versus Sham; $^{###}P \leq 0.001$ versus TMEV-VEH animals (non-parametric Kruskal–Wallis test): Scale bar = 5 µm; 100 µm.

infected animals that received the vehicle alone, yet it was absent in the Sham mice. Treatment with Sativex restored Neurofilament-H staining (Figure 5B), reflecting the preservation of the axonal package (Figure 5C). Similarly, the axonal swelling evident when longitudinal spinal cord sections of TMEV-infected animals that received the vehicle alone were stained with Neurofilament-H (Figure 6A) was less frequent and milder following Sativex administration, as confirmed in longitudinal spinal cord sections labelled with SMI32 (Figure 6B).

Sativex reduced astrocyte reactivity and the accumulation of CSPGs in the spinal cord of TMEV-infected mice

To address whether the treatment with Sativex affected astrogliosis and the expression of CSPGs in TMEV-IDD at the chronic phases of the disease, we analysed its effects on astroglial reactivity using GFAP and vimentin staining as an indicator of reactive astrocytes (Nash *et al.*, 2011). Likewise, the accumulation of CSPGs was studied by staining with

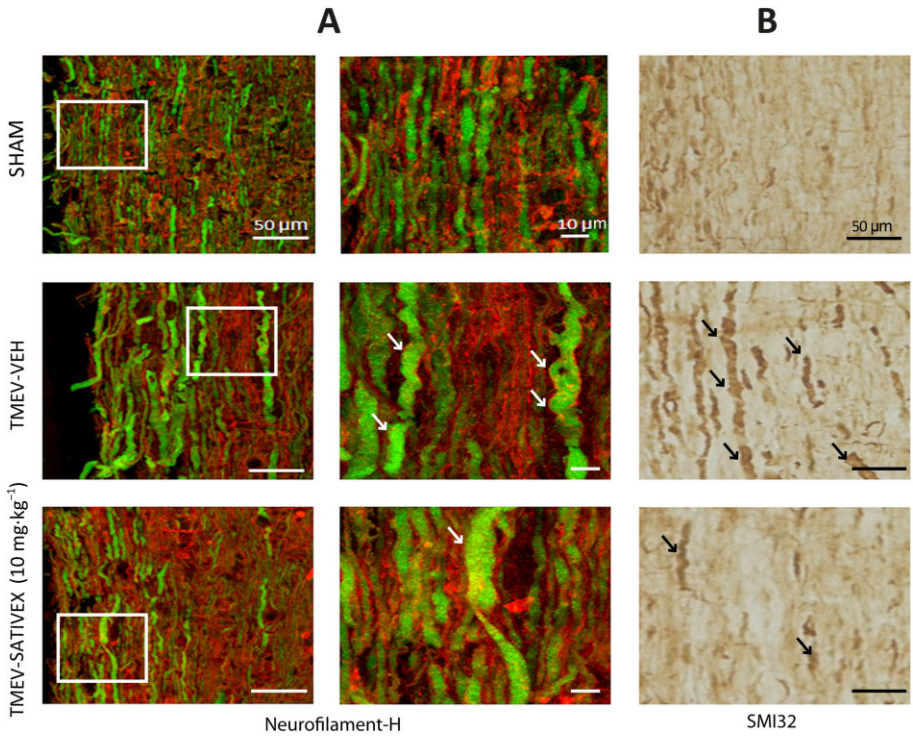

Figure 6

A Sativex®-like phytocannabinoid combination prevented the swelling and ovoid formations in axons from TMEV-infected animals. Longitudinal cervical spinal cord sections (30 µm thick) stained for Neurofilament-H (green) and RIP (red) (A) revealed the axons to be swollen, deformed and with ovoid formation in TMEV vehicle-treated mice. Lesions in the axons of the Sativex-treated group (10 mg·kg^{-1}) were less frequent and axons displayed markedly reduced damage as confirmed in longitudinal spinal cord sections labelled with SMI32 (B): Scale bar = 10 µm; 50 µm.

CS56 and analysing the brevican gene expression in the spinal cord. There was prominent astrogliosis [Figure 7: GFAP (A,B) and vimentin (C) staining] associated with the accumulation of CSPGs (CS56) in the spinal cord of vehicle-treated TMEV-infected mice (Figure 7D). However, treatment with Sativex reduced both astrogliosis (Figure 7B) CS56 staining (Figure 7D) and brevican gene expression (Figure 7E) in TMEV-infected mice, suggesting that it may modulate glial scar formation.

Sativex reduced CSPGs synthesis and release by astrocytes in vitro

As astrocytes are the main source of CSPGs (Susarla *et al.*, 2011), we assessed the capability of Sativex to alter the production of CSPGs by astrocytes in culture. Exposure to the Sativex not only reduced the mRNA expression of brevican and XT-I in activated astrocytes (TGFβ1 and bFGF) after 24 h (Figure 8A), but it also reduced the neurocan protein staining at an intracellular and extracellular level in astrocytes by immunocytochemistry (Figure 8B). Most importantly, Sativex diminished the release of neurocan by activated astrocytes when assessed at 72 h (Figure 8C,D). An overall inhibitory effect of Sativex on CSPG production by astrocytes occurred at a dose of 0.50 µM. However, a dose of 100 nM (50 nM for each phytocannabinoid) also achieved a significant reduction in the expression of brevican mRNA and the dose of 1.0 µM (0.5 µM for each phytocannabinoid) diminished the expression of XT-I mRNA within 24 h. Together, these data suggest that astrocytes could represent a new target for Sativex activity, modulating the production of CSPG.

Discussion

Despite intense research, there are still no treatments available to achieve clinical modification of progressive MS. The approval of Sativex for treatment of spasticity and neuropathic pain in MS opens the door to study the therapeutic potential of Sativex as a disease-modifying agent. Accordingly, we have assessed the efficacy of Sativex in controlling disease progression in a model of primary progressive MS, the TMEV-IDD model (Mecha *et al.*, 2013a).

There is a wealth of data from clinical trials that support the efficacy and safety of Sativex in patients with MS-related spasticity (Collin *et al.*, 2007; Wade *et al.*, 2010; Sastre-Garriga *et al.*, 2011; García-Merino, 2013). However, to date, there are no clinical studies evaluating Sativex as a disease-modifying agent of progressive MS. The closest clinical study is the CUPID trial, the results of which were recently published (Zajicek *et al.*, 2013). This study showed that dronabinol (Δ^9-THC) administration to patients with progressive MS did not slow the course of the disease. However, the failure to detect

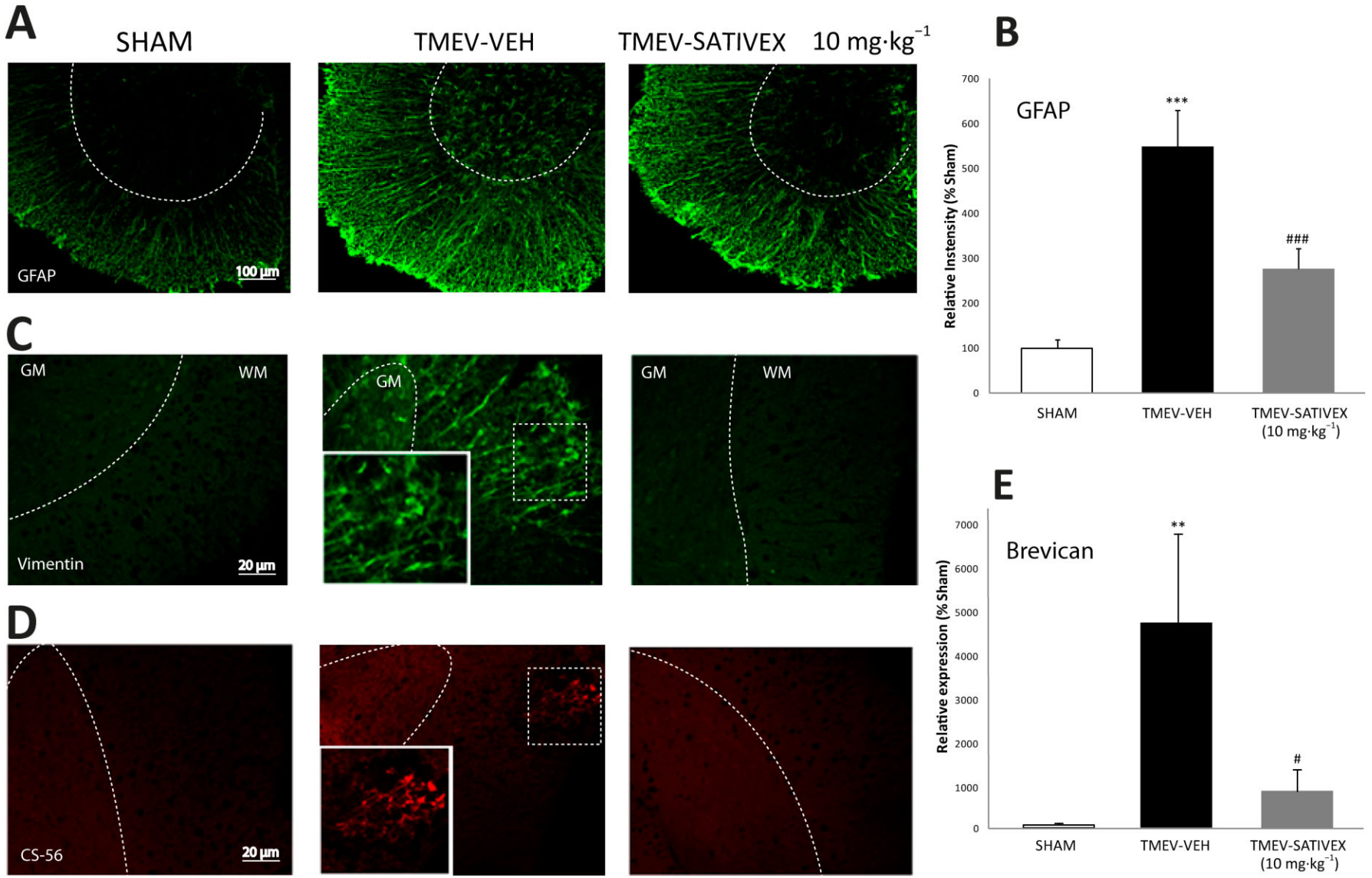

Figure 7

A Sativex®-like phytocannabinoid combination reduced astrocyte reactivity and the accumulation of CSPGs. Transverse cervical spinal cord sections (30 µm) were obtained on day 80 post-infection and stained for GFAP, vimentin and CS56. There was a prominent astrogliosis in the spinal cord of vehicle-treated infected animals evident in the representative microphotographs of GFAP staining (A). This is also reflected in the area occupied by GFAP$^+$ astrocytes in the spinal cord white matter in each field (5–6 slices, n = 5–6 animals per group) (B), as well as in the vimentin staining (C). This astrogliosis is associated with an accumulation of CSPGs (CS56 staining, D; brevican gene expression, E) which is impeded by Sativex treatment (10 mg·kg^{-1}). The data represent the mean ± SEM: **$P \leq 0.01$, ***$P \leq 0.001$ versus Sham; #$P \leq 0.05$, ###$P \leq 0.001$ versus TMEV-VEH animals (one-way ANOVA followed by Tukey's and Bonferroni test: GFAP analysis; Non parametric Kruskal–Wallis test: brevican). WM, white matter; GM, gray matter. Scale bar = 100 µm; 20 µm.

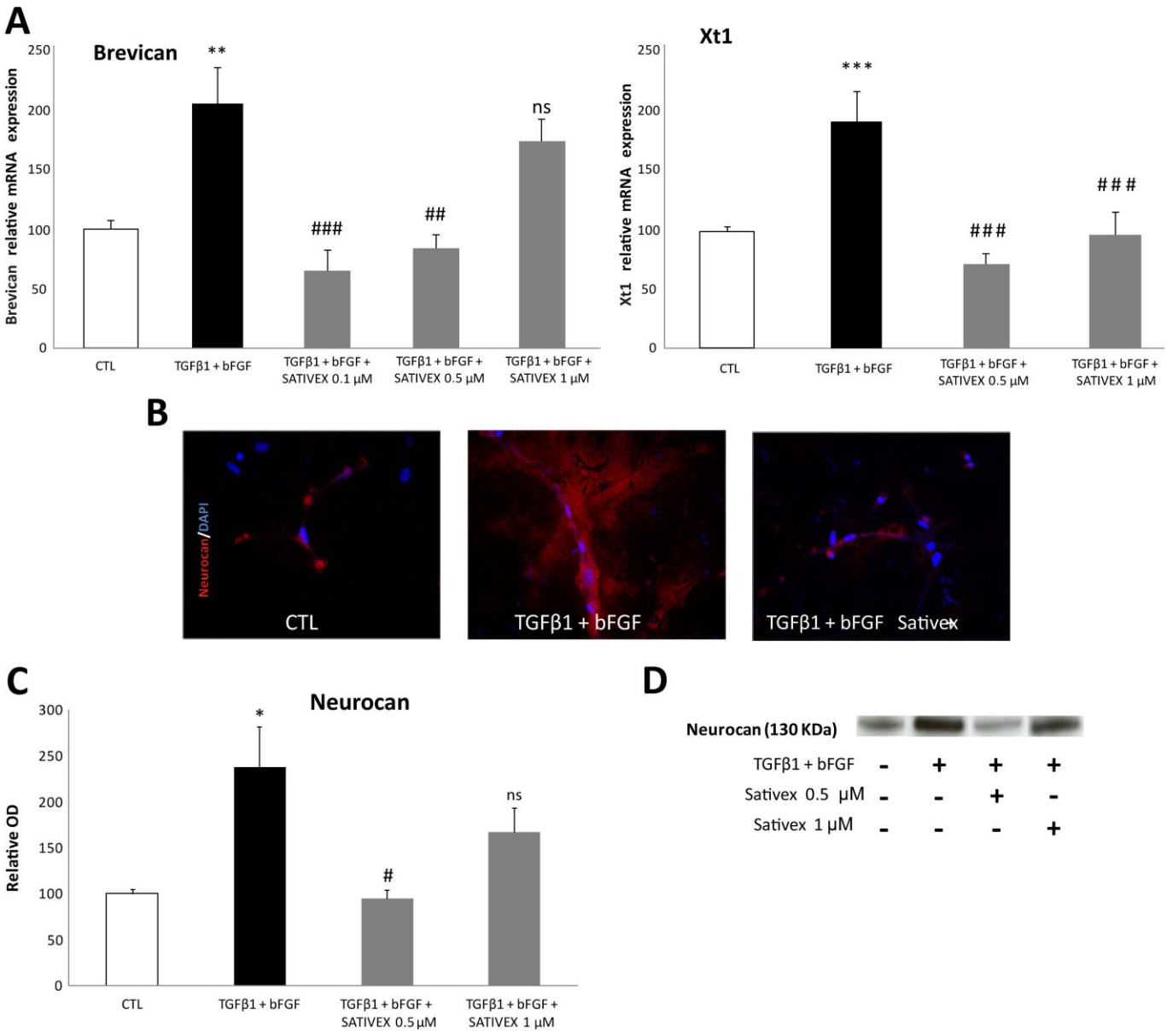

Figure 8

A Sativex®-like phytocannabinoid combination treatment reduced the synthesis and release of CSPGs by astrocytes *in vitro*. CSPG, brevican and XT-I enzyme syntheses are up-regulated in primary rat astrocytes stimulated with TGFβ1 (10 ng·mL^{-1}) plus bFGF (10 ng·mL^{-1}) and significantly down-regulated by Sativex at a dose of 100 nM and 0.5 µM or 1 µM in the case of XT-I after 24 h of treatment. Brevican and XT-I mRNA induction was determined by RT-PCR, normalizing mRNA expression (n = 10 per group) to that of the 18S gene (A). Representative microphotographs of primary astrocytes after 48 h in the presence of Sativex (0.5 µM) show that neurocan immunocytochemistry is less intense than in control astrocytes, both at the intracellular level and in the culture substrate (B). In the presence of Sativex (0.5 µM) for 72 h, activated astrocytes release less neurocan to the supernatant, as evident in Western blots. Representative Western blots (C) and quantification of the OD (D). Every assay was performed in duplicate, in three independent experiments. The data represent the mean ± SEM: *$P \leq 0.05$, **$P \leq 0.01$, ***$P \leq 0.001$ versus CTL (control); #$P \leq 0.05$, ##$P \leq 0.01$, ###$P \leq 0.001$ versus TGFβ1+ bFGF (non-parametric Kruskal–Wallis test). ns, not significant.

such an effect may reflect the high attrition rate and the lower rate of disease progression than initially expected.

The study performed here is the first to address the effect of Sativex on primary progressive MS in a recognized experimental model, providing highly promising results in terms of reduced axonal damage. Indeed, this result is consistent with the proposed neuroprotective profile of Sativex and its components (Valdeolivas *et al.*, 2012; Moreno-Martet *et al.*, 2014). When administered alone, Δ^9-THC or CBD has positive effects on disease progression in EAE, CREAE and TMEV-IDD models. A clinical and histological improvement provoked by Δ^9-THC, predominantly reducing inflammation, was first described in EAE rats (Lyman *et al.*, 1989). Here, we also found that Δ^9-THC-BDS ameliorated the progression of

disease in TMEV-IDD mice, with a major participation of CB_1 receptors, even though blocking CB_2 receptors partly prevented the benefits elicited by this phytocannabinoid. The activation of CB_1 receptors probably mediates the neuroprotective effects of Δ^9-THC as this receptor fulfils an important role in the defence against excitotoxicity (Marsicano *et al.*, 2003) and excitotoxic mechanisms are prominent in TMEV-IDD (Docagne *et al.*, 2007). Nevertheless, the participation of CB_2 receptors is not unexpected given their key involvement in the control of glial activation and given that inflammatory events are also important in TMEV-IDD mice (Arévalo-Martín *et al.*, 2003; 2008). Indeed, it was previously demonstrated that Δ^9-THC suppressed CNS autoimmune inflammation with the participation of both CB_1 and CB_2 receptors in CREAE mice (Maresz *et al.*, 2007).

With regard to CBD, the other component of Sativex, this phytocannabinoid provokes a reduction in disease severity in both autoimmune (EAE mice) and viral (TMEV-IDD mice) models of MS, as well as in a murine collagen-induced arthritis model (Malfait *et al.*, 2000; Kozela *et al.*, 2011; Mecha *et al.*, 2013b). The attenuation of disease progression in MS models involved the reduction of immune cell infiltrates and the decrease in microglial activation following systemic CBD treatment (5 $mg{\cdot}kg^{-1}$), the same dose of CBD-BDS used in this study. These findings contrast with the earlier failure to find an effect of CBD in the CREAE model of MS (Maresz *et al.*, 2007), which might reflect differences in the strain of mice and/or in the antigen used. The influence of genetic background on EAE in mice deficient in some key endocannabinoid genes has recently been shown (Sisay *et al.*, 2013). It should be noted that CBD is not particularly active at classic CB_1 and CB_2 receptors and, while it appears to be able to inhibit the inactivation of endocannabinoids (Bisogno *et al.*, 2001), its mechanisms of action are quite diverse and extend to targets beyond the cannabinoid system (see Fernández-Ruiz *et al.*, 2013). One of these targets includes the nuclear receptors of the PPAR family, in particular PPARγ (O'Sullivan and Kendall, 2010; Esposito *et al.*, 2011). Here, we found that the inhibition of PPARγ completely blocked the motor benefits of CDB-BDS, clearly indicating the participation of these nuclear receptors in the effects of CBD-BDS on TMEV-IDD and presumably when it is combined with Δ^9-THC-BDS in Sativex. This is consistent with studies showing that activation of PPARγ by selective agonists ameliorated MS symptomatology (Feinstein *et al.*, 2002; Klotz *et al.*, 2009; Mestre *et al.*, 2009).

In accordance with the diminished axonal damage, we found reduced astrogliosis and CSPGs accumulation during the late chronic phase of TMEV-IDD. It is well known that CPGSs are up-regulated in demyelinated MS lesions (Haylock-Jacobs *et al.*, 2011; Haist *et al.*, 2012). In particular, astrocytes at the edge of active MS lesions up-regulate CSPGs such as versican, aggrecan and neurocan (Haylock-Jacobs *et al.*, 2011; Haist *et al.*, 2012; Lau *et al.*, 2012). Significantly, there are several *in vitro* studies indicating that neurocan and aggrecan impair the outgrowth of oligodendrocyte process, OPC differentiation and myelination (Siebert and Osterhout, 2011; Pendleton *et al.*, 2013). Here, the enhanced expression of CSPGs in astrocytes following exposure to TGFβ (Gris *et al.*, 2007; Susarla *et al.*, 2011) was down-regulated by Sativex administration. We focused on neurocan and brevican, core proteins that carry inhibitory glycosaminoglycan (GAG) chains. CSPG side chain synthesis is initiated by the addition of xylose to a serine moiety of the core protein, a step carried out by XT-I, among other enzymes (Gris *et al.*, 2007). Significantly, the up-regulation of XT-I expression in stimulated astrocytes was dampened by Sativex, which could impair CSPG synthesis and thereby provide a permissive environment for regeneration in accordance with previous studies in which XT-I targeting promotes neurite outgrowth (Hurtado *et al.*, 2008).

The inhibitory effect of Sativex in the production of brevican and neurocan as well as in the synthesis enzyme XT-I by activated astrocytes confirm our *in vivo* results and support the interest of Sativex as a putative therapy in promoting repair myelin processes by reducing astroglial scar. Further work is necessary to delineate the effects of Sativex-like combination of phytocannabinoids on remyelination in experimental models of MS.

In conclusion, Sativex improved the neurological deficits evident at the chronic phases of the TMEV-IDD model of MS. These effects were fully reproduced by CBD-BDS alone, acting through PPARγ and, to a lesser extent, by Δ^9-THC-BDS, acting through CB_2 and primarily CB_1 receptors. One potential explanation for the beneficial effects of Sativex could be the reduced transmigration of cell infiltrates into the parenchyma. Sativex also acted as an immunomodulator, decreasing microglial reactivity, the expression of proinflammatory cytokine genes and increasing levels of Arg-1 and IL-10. Moreover, Sativex diminished axonal damage and restored myelin morphology, again supporting its cytoprotective potential. Finally, we postulate that Sativex could modulate glial scar formation, reducing astrogliosis and the accumulation of CSPGs *in vivo*, as well as in astrocyte cultures. As CSPGs associated with inflammation have been implicated in the failure of remyelination in human MS and in murine models of demyelination, our results highlight the potential benefits of Sativex in CNS repair.

Acknowledgements

This work was supported by grants from the Ministry of the Economy and Competition SAF2010-17501 (C. G.) and SAF2009-11847 (J. F.-R.), the Comunidad de Madrid, S2011/BMD-2308, the Red Española de Esclerosis Múltiple RD12/0032/0008 (C. G.) sponsored by the Fondo de Investigación Sanitaria. GW Pharmaceuticals Ltd provided the combination of phytocannabinoids. None of the funding bodies played any role in the study design, data collection and analysis, the decision to publish or the preparation of the manuscript.

Author contributions

A. F. carried out the TMEV-IDD model, prepared the astrocytes cultures, determined the ECM proteins and analysed the data. M. M. performed the qRT-PCR assays. M. M.-M. was involved in motor tests. F. J. C.-S. was involved in perfusion and sections staining. M. M.-M., E. L., J. F.-R. and C. G. participated in the experimental design. A. F. and C. G. wrote the manuscript.

Conflict of interest

The authors have formal links with GW Pharmaceuticals that fund some of their research.

References

Alexander SPH, Benson HE, Faccenda E, Pawson AJ, Sharman JL, Spedding M *et al*. (2013a). The Concise Guide to PHARMACOLOGY 2013/14: G Protein-Coupled Receptors. Br J Pharmacol 170: 1459–1581.

Alexander SPH, Benson HE, Faccenda E, Pawson AJ, Sharman JL, Spedding M *et al*. (2013b). The Concise Guide to PHARMACOLOGY 2013/14: Nuclear Hormone Receptors. Br J Pharmacol 170: 1652–1675.

Alexander SPH, Benson HE, Faccenda E, Pawson AJ, Sharman JL, Spedding M *et al*. (2013c). The Concise Guide to PHARMACOLOGY 2013/14: Enzymes. Br J Pharmacol 170: 1797–1867.

Arévalo-Martín A, Vela JM, Molina-Holgado E, Borrell J, Guaza C (2003). Therapeutic action of cannabinoids in a murine model of multiple sclerosis. J Neurosci 23: 2511–2516.

Arévalo-Martín A, García-Ovejero D, Gómez O, Rubio-Araiz A, Navarro-Galve B, Guaza C *et al*. (2008). CB2 cannabinoid receptors as an emerging target for demyelinating diseases: from neuroimmune interactions to cell replacement strategies. Br J Pharmacol 153: 216–225.

Baker D, Pryce G, Croxford JL, Brown P, Pertwee RG, Huffman JW *et al*. (2000). Cannabinoids control tremor and spasticity in a multiple sclerosis model. Nature 404: 84–87. 6773.

Bisogno T, Hanus L, De Petrocellis L, Tchilibon S, Ponde DE, Brandi I *et al*. (2001). Molecular targets for cannabidiol and its synthetic analogues: effects on vanilloid VR1 receptors and on the cellular uptake and enzymatic hydrolysis of anandamide. Br J Pharmacol 134: 845–852.

Chang A, Tourtellotte WW, Rudick R, Trapp BD (2002). Premyelinating oligodendrocytes in chronic lesions of multiple sclerosis. N Engl J Med 346: 165–173.

Chang A, Staugaitis SM, Dutta R, Batt CE, Easley KE, Chomyk AM *et al*. (2012). Cortical remyelination: a new target for repair therapies in multiple sclerosis. Ann Neurol 72: 918–926.

Collin C, Davies P, Mutiboko IK, Ratcliffe S, Sativex Spasticity in MS Study Group (2007). Randomized controlled trial of cannabis-based medicine in spasticity caused by multiple sclerosis. Eur J Neurol 14: 290–296.

Compston A, Coles A (2008). Multiple sclerosis. Lancet 372: 1502–1517.

Croxford JL, Miller SD (2003). Immunoregulation of a viral model of multiple sclerosis using the synthetic cannabinoid R + WIN55,212. J Clin Invest 111: 1231–1240.

Docagne F, Muñetón V, Clemente D, Ali C, Loría F, Correa F *et al*. (2007). Excitotoxicity in a chronic model of multiple sclerosis: neuroprotective role of cannabinoids through CB1 and CB2 receptor activation. Mol Cell Neurosci 34: 551–561.

Esposito G, Scuderi G, Valenza M, Togna GI, Latina V, De Filippis D *et al*. (2011). Cannabidiol reduces Ab-induced neuroinflammation and promotes hippocampal neurogenesis through PPARγ involvement. PLoS ONE 6: e28668.

Feinstein DL, Galea E, Gavrilyuk V, Brosnan CF, Whitacre CC, Dumitrescu-Ozimek L *et al*. (2002). Peroxisome proliferator-activated receptor gamma agonists prevent experimental autoimmune encephalomyelitis. Ann Neurol 51: 694–702.

Fernández-Ruiz J, García C, Sagredo O, Gómez-Ruiz M, de Lago E (2010). The endocannabinoid system as a target for the treatment of neuronal damage. Expert Opin Ther Targets 14: 387–404.

Fernández-Ruiz J, Sagredo O, Pazos MR, García RG, Pertwee R, Mechoulam R *et al*. (2013). Cannabidiol for neurodegenerative disorders: important new clinical applications for this phytocannabinoid. Br J Clin Pharmacol 75: 323–333.

Franklin RJM (2002). Why does remyelination fail in multiple sclerosis? Nat Rev Neurosci 3: 705–714.

García-Merino A (2013). Endocannabinoid system modulator use in everyday clinical practice in the UK and Spain. Expert Rev Neurother 13: 9–13.

Gómez O, Arevalo-Martin A, Garcia-Ovejero D, Ortega-Gutierrez S, Cisneros JA, Almazan G *et al*. (2010). The constitutive production of 2-arachidonoylglycerol participates in oligodendrocyte differentiation. Glia 58: 1913–1927.

Goldschmidt T, Antel J, König FB, Brück W, Kuhlmann T (2009). Remyelination capacity of the MS brain decreases with disease chronicity. Neurology 72: 1914–1921.

Gris P, Tighe A, Levin D, Sharma R, Brown A (2007). Transcriptional regulation of scar gene expression in primary astrocytes. Glia 55: 1145–1155.

Haist V, Ulrich R, Kalkuhl A, Deschl U, Baumgartner W (2012). Distinct spatio-temporal extracellular matrix accumulation within demyelinated spinal cord lesions in Theiler's murine encephalomyelitis. Brain Pathol 22: 188–204.

Harlow DE, Macklin WB (2014). Inhibitors of myelination: ECM changes, CSPGs and PTPs. Exp Neurol 251: 39–46.

Haylock-Jacobs S, Keough MB, Lau L, Yong VW (2011). Chondroitin sulphate proteoglycans: extracellular matrix proteins that regulate immunity of the central nervous system. Autoimmun Rev 10: 766–772.

Hurtado A, Podinin H, Oudega M, Grimpe B (2008). Deoxyribozyme-mediated knockdown of xylosyltransferase-1 mRNA promotes axon growth in the adult rat spinal cord. Brain 131: 2596–2605.

Izzo AA, Borrelli F, Capasso R, Di Marzo V, Mechoulam R (2009). Non-Psychotropic plant cannabinoids: new therapeutic opportunities for an ancient herb. Trends Pharmacol Sci 30: 515–527.

Kilkenny C, Browne W, Cuthill IC, Emerson M, Altman DG (2010). Animal research: Reporting *in vivo* experiments: the ARRIVE guidelines. Br J Pharmacol 160: 1577–1579.

Klotz L, Burgdorf S, Dani I, Saijo K, Flossdorf J, Hucke S *et al*. (2009). The nuclear receptor PPAR gamma selectively inhibits Th17 differentiation in a T cell intrinsic fashion and suppresses CNS autoimmunity. J Exp Med 206: 2079–2089.

Kozela E, Lev N, Kaushansky N, Eilam R, Rimmerman N, Levy R *et al*. (2011). Cannabidiol inhibits pathogenic T cells, decreases spinal microglial activation and ameliorates multiple sclerosis-like disease in C57BL/6 mice. Br J Pharmacol 163: 1507–1519.

Lau LW, Keough MB, Haylock-Jacobs S, Cua R, Döring A, Sloka S *et al*. (2012). Chondroitin sulfate proteoglycans in demyelinated lesions impair demyelination. Ann Neurol 72: 419–432.

Lipton HL, Dal Canto MC (1976). Chronic neurologic disease in Theiler's virus infection of SJL/J mice. J Neurol Sci 30: 201–207.

Lledó A, Borrell J, Guaza C (1999). Dexamethasone regulation of interleukin-1 receptors in the hippocampus of Theiler's virus infected mice: effects on virus-mediated demyelination. Eur J Pharmacol 372: 75–83.

Loría F, Petrosino S, Hernangómez M, Mestre L, Spagnolo A, Correa F *et al*. (2010). An endocannabinoid tone limits excitotoxicity *in vitro* and in a model of multiple sclerosis. Neurobiol Dis 37: 166–176.

Lyman WD, Sonett JR, Brosnan CF, Elkin R, Bornstein MB (1989). Delta 9-tetrahydrocannabinol: a novel treatment for experimental autoimmune encephalomyelitis. J Neuroimmunol 23: 73–81.

Malfait AM, Gallily R, Sumariwalla PF, Malik AS, Andreakos E, Mechoulam R *et al*. (2000). The non-psychotropic cannabis constituent cannabidiol is an oral anti-arthritic therapeutic in murine collagen-induced arthritis. Proc Natl Acad Sci USA 97: 9561–9566.

Maresz K, Pryce G, Ponomarev ED, Marsicano G, Croxford JL, Shriver LP *et al*. (2007). Direct suppression of CNS autoimmune inflammation via the cannabinoid receptor CB1 on neurons and CB2 on autoreactive T cells. Nat Med 13: 492–497.

Marsicano G, Goodenough S, Monory K, Hermann H, Eder M, Cannich A *et al*. (2003). CB1 cannabinoid receptors and on demand defense against excitotoxicity. Science 302: 84–88.

McGrath J, Drummond G, McLachlan E, Kilkenny C, Wainwright C (2010). Guidelines for reporting experiments involving animals: the ARRIVE guidelines. Br J Pharmacol 160: 1573–1576.

Mecha M, Iñigo PM, Mestre L, Hernangómez M, Borrel J, Guaza C (2011). An easy and fast way to obtain a high number of glial cells from rat cerebral tissue: a beginners approach. Protoc Exch. doi: 10.1038/protex.2011.218

Mecha M, Torrao AS, Mestre L, Carrillo-Salinas FJ, Mechoulam R, Guaza C (2012). Cannabidiol protects oligodendrocyte progenitor cells from inflammation-induced apoptosis by attenuating endoplasmic reticulum stress. Cell Death Dis 3: e331.

Mecha M, Carrillo-Salinas FJ, Feliu A, Guaza C (2013a). Viral models of multiple sclerosis: neurodegeneration and demyelination in mice infected with Theiler's virus. Prog Neurobiol 102: 46–64.

Mecha M, Feliú A, Iñigo PM, Mestre L, Carrillo-Salinas FJ, Guaza C (2013b). Cannabidiol provides long-lasting protection against the deleterious effects of inflammation in a viral model of multiple sclerosis: a role for A2A receptors. Neurobiol Dis 59: 141–150.

Mestre L, Docagne F, Correa F, Loría F, Hernangómez M, Borrell J *et al*. (2009). A cannabinoid agonist interferes with the progression of a chronic model of multiple sclerosis by downregulation the adhesion molecules. Mol Cell Neurosci 40: 258–266.

Miller SD, Vanderlugt CL, Begolka WS, Pao W, Yauch RL, Neville KL *et al*. (1997). Persistent infection with TMEV leads to CNS autoimmunity via epitope spreading. Nat Med 3: 1133–1136.

Mohan H, Krumbholz M, Sharma R, Eisele S, Junker A, Sixt M *et al*. (2010). *E*xtracellular matrix in multiple sclerosis lesions: fibrillar collagens, biglycan and decorin are upregulated and associated with infiltrating immune cells. Brain Pathol 20: 966–975.

Molina-Holgado E, Vela JM, Arévalo-Martín A, Almazán G, Molina-Holgado F, Borrell J *et al*. (2002). Cannabinoids promote oligodendrocyte progenitor survival: involvement of cannabinoid receptors and phosphatidylinositol-3 kinase/Akt signaling. J Neurosci 22: 9742–9753.

Moreno-Martet M, Espejo-Porras F, Fernández-Ruiz J, de Lago E (2014). Changes in endocannabinoid receptors and enzymes in the spinal cord of SOD1G93A transgenic mice and evaluation of a Sativex®-like combination of phytocannabinoids: interest for future therapies in amyotrophic lateral sclerosis. CNS Neurosci Ther 20: 809–815.

Nash B, Ioannidou K, Barnett SC (2011). Astrocyte phenotypes and their relationship to myelination. J Anat 219: 44–52.

O'Sullivan SE, Kendall DA (2010). Cannabinoid activation of peroxisome proliferator-activated receptors: potential for modulation of inflammatory disease. Immunobiology 215: 611–616.

Pawson AJ, Sharman JL, Benson HE, Faccenda E, Alexander SP, Buneman OP *et al*.; NC-IUPHAR. (2014). The IUPHAR/BPS Guide to PHARMACOLOGY: an expert-driven knowledge base of drug targets and their ligands. Nucl Acids Res 42 (Database Issue): D1098–D1106.

Pendleton JC, Shamblott MJ, Gary DS, Belegu V, Hurtado A, Malone ML *et al*. (2013). Chondroitin sulfate proteoglycans inhibit oligodendrocyte myelination through PTPσ. Exp Neurol 247: 113–121.

Pryce G, Baker D (2012). Potential control of multiple sclerosis by cannabis and the endocannabinoid system. CNS Neurol Disord Drug Targets 11: 624–641.

Pryce G, Ahmed Z, Hankey DJ, Jackson SJ, Croxford JL, Pocock JM *et al*. (2003). Cannabinoids inhibit neurodegeneration in models of multiple sclerosis. Brain 126: 2191–2202.

Sastre-Garriga J, Vila C, Clissold S, Montalban X (2011). THC and CBD oromucosal spray (Sativex®) in the management of spasticity associated with multiple sclerosis. Expert Rev Neurother 11: 627–637.

Serpell MG, Notcutt W, Collin C (2013). Sativex long-term use: an open-label trial study in patients with spasticity due to multiple sclerosis. J Neurol 260: 285–295.

Siebert JR, Osterhout DJ (2011). The inhibitory effects of chondroitin sulfate proteoglycans on oligodendrocytes. J Neurochem 119: 176–188.

Silver J, Miller JH (2004). Regeneration beyond the glial scar. Nat Rev Neurosci 5: 146–156.

Sisay S, Pryce G, Jackson SJ, Tanner C, Ross RA, Michael GJ *et al*. (2013). Genetic background can result in a marked or minimal effect of gene knockout (GPR55 and CB2 receptor) in experimental autoimmune encephalomyelitis models of multiple sclerosis. PLoS ONE 8: e76907.

Sobel RA, Ahmed AS (2001). White matter extracellular matrix chondroitin sulfate/dermatan sulfate proteoglycans in multiple sclerosis. J Neuropathol Exp Neurol 60: 1198–1207.

Susarla BT, Laing ED, Yu P, Katagiri Y, Geller HM, Symes AJ (2011). Smad proteins differentially regulate transforming growth factor-β-mediated induction of chondroitin sulfate proteoglycans. J Neurochem 119: 868–878.

Ulrich R, Seeliger F, Kreutzer M, Germann PG, Baumgärtner W (2008). Limited remyelination in Theiler's murine encephalomyelitis due to insufficient oligodendroglial differentiation of nerve/glial antigen 2 (NG2)-positive putative oligodendroglial progenitor cells. Neuropathol Appl Neurobiol 34: 603–620.

Valdeolivas S, Satta V, Pertwee RG, Fernández-Ruiz J, Sagredo O (2012). Sativex like combination of phytocannabinoids is neuroprotective in malonate-lesioned rats, an inflammatory model of Hungtinton's disease: role of CB1 and CB2 receptors. ACS Chem Neurosci 3: 400–406.

Velayudhan L, Van Diepen E, Marudkar M, Hands O, Suribhatla S, Prettyman R *et al*. (2014). Therapeutic potential of cannabinoids in neurodegenerative diseases: a selective review. Curr Pharm Des 20: 2218–2230.

Wade DT, Collin C, Stott C, Duncombe P (2010). Meta-analysis of the efficacy of Sativex (nabiximols), on spasticity in people with multiple sclerosis. Mult Scler 16: 707–714.

Zajicek J, Ball S, Wright D, Vickery J, Nunn A, Miller D *et al*. (2013). Effect of dronabinol on progression in progressive multiple sclerosis (CUPID): a randomised, placebo-controlled trial. Lancet Neurol 12: 857–865.